ACS APPLIED MATERIALS & INTERFACES

www.acsami.org

Research Article

Effects of Environmental Temperature and Trapped Air Bubbles on the Mechanical Properties of Ice Cubes

Keke Shao, Mengjie Song,* Biaohua Cai, Long Zhang, Libor Pekař, and Xuan Zhang*

Cite This: *ACS Appl. Mater. Interfaces* 2024, 16, 63482−63494

Read Online

ACCESS | Metrics & More | Article Recommendations | Supporting Information

ABSTRACT: Ice is a widespread material in natural and industrial fields. Trapped air bubbles form in ice cubes due to the differences in the solubility of air in ice and water, which directly affects the mechanical strength of the ice cubes. To investigate the effects of environmental temperature and trapped air bubbles on the mechanical properties of ice cubes, a series of experiments are designed and carried out. A mathematical model that predicts the mechanical strength of ice cubes with an accuracy over 80% is developed and validated. The results show that even a volume content of trapped air bubbles in an ice cube as low as 1.98% can greatly impact the mechanical properties. This model reveals the mechanisms and principles governing the influences of environmental temperature and bubble volume content on the mechanical strength of ice cubes. As the environmental temperature decreases from 0 to −20 °C, the compressive strength of clear ice cubes increases from 1.71 to 2.10 MPa, while that of bubble ice cubes increases from 1.58 to 1.95 MPa. This study has implications for utilizing trapped air bubbles to regulate the mechanical properties of ice and for optimizing various mechanical deicing techniques.

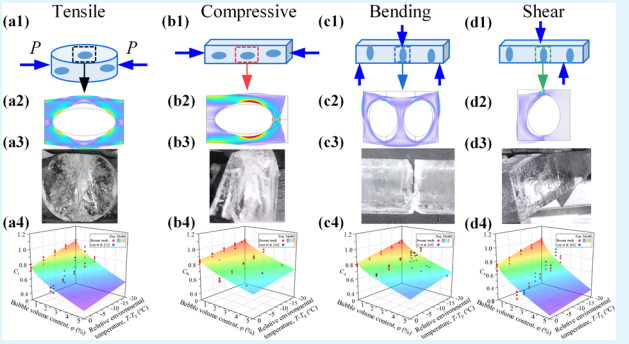

KEYWORDS: *Ice cube, Trapped air bubble, Mechanical property, Environmental temperature, Bubble volume content*

1. INTRODUCTION

Icing on various device surfaces is a common liquid−solid phase change process that occurs in low temperature and high humidity environments,[1,2] which causes numerous problems in areas of power generation,[3,4] aerospace,[5] transportation,[6,7] air-conditioning,[8,9] and refrigeration,[10] and thus reduces the efficiency of equipment operation reduced and leading to significant financial losses.[11,12]. To avoid problems caused by icing, both active and passive deicing techniques have been employed in applications.[13,14] The active deicing methods include heating, mechanical removal, and liquid spraying, while the passive ones include functional surfaces and coatings, such as superhydrophobic or slippery ones.[15,16] Active deicing is energy intensive, while passive deicing is less energy intensive but also less efficient. To optimize various mechanical active deicing techniques and reduce deicing energy consumption, it is necessary to study the mechanical properties of ice and their influencing factors.

Traditional research on the mechanical properties of ice has focused on its tensile, compressive, bending, and shear mechanical features of ice[17] carried out by experimental methods,[18,19] numerical simulations,[20] mathematical modeling,[21] and even by using artificial intelligence.[22,23] Experimental methods are the most common way to study the mechanical properties of ice. Experimental results suggest that ice is always damaged by longitudinal cracks along the loading direction,[24,25] thus the damage pattern of ice is mainly dominated by tensile and compressive damage. The bending feature of ice such as ice fracture toughness is commonly measured by the three-point bend test.[26] Under passively restrained triaxial compressive loading with high strain rates, ice damage cracks form and develop along the 45° direction of the load. This reveals that the ice damage also exhibits shear damage modes at certain specific stress states.[27,28] The mechanical properties are also affected by the strain rate and environmental temperature. When the strain rate increases from 10^{-6} to 10^{-3} s^{-1}, the mechanical properties of the ice change from hard to brittle.[29,30]

In addition to the research methods of ice mechanical properties being investigated, the parameters affecting the mechanical properties of ice have been studied extensively. Icing occurs when the water temperature drops below the freezing point,[31,32] and is influenced by other conditions such as temperature, surface wettability, solute, fillers, and environmental pressure.[33,34] Specially, due to the significantly lower

Received: July 22, 2024
Revised: October 8, 2024
Accepted: October 8, 2024
Published: November 7, 2024

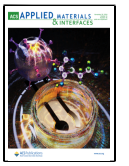

solubility of air in ice than that in water, dissolved air is squeezed out of the ice during icing and accumulates near the freezing front.[35,36] Once the air concentration reaches a critical saturation, air bubbles nucleate and are trapped in ice.[37,38] The bubble size and distribution depend on the icing rate, amount of dissolved air, and environmental pressure.[39,40] The uniaxial compressive strength of ice is inversely proportional to the porosity.[41,42] The dynamic strength of bubble ice decreases nonlinearly with increasing porosity. Both the porosity and the distribution of bubbles in ice affect the dynamic strength at low strain rate levels, but the distribution rarely affects the dynamic strength at high strain rate levels.[43−45] The slope of the load−displacement curve increases with increasing fiber content until the maximum compression force is reached, and then the force decreases rapidly, indicating a rapid decrease in the strength of the ice.[46,47] Besides, it has been found that the ice grain size and specimen volumes affect the mechanical properties.[48,49]

Previous works have conducted a lot of research on the effect of strain rate,[50] environmental temperature,[30] porosity,[42] and grain size[48] on the mechanical properties of ice. The effect of a single influencing factor on the mechanical properties of ice has been studied extensively, but the effect of coupled factors has rarely been taken seriously. Few of them comprehensively discussed the coupling effect of these factors on the mechanical properties of ice.[51] However, real ice is often encountered with complex conditions and the combined effects of multiple factors. In addition, the relationship between the ice formation process and the mechanical properties has been rarely investigated, especially the effect of trapped air bubbles in the ice. Since air is always dissolved in water, the appearance of trapped bubbles in ice is inevitable.[39] Trapped air bubbles are defects, which lead to stress concentration and thus affect the mechanical strength of ice.[42] Moreover, environmental temperature could change the morphology of bubbles as well as the mechanical properties of ice.[52]

In this study, an ice-making experimental setup is constructed to prepare clear ice cubes with no bubbles and bubble ice cubes with a uniform distribution of trapped air bubbles. A experimental setup for mechanical test is also built to measure the tensile, compressive, bending, and shear properties of clear and bubble ice cubes. The coupling effects of environmental temperature and bubble content on the stiffness, strength, and modulus of ice are discussed with a mathematical model developed. This study has implications for regulating the mechanics properties of ice and optimizing various mechanical deicing techniques relying on trapped air bubbles.

2. EXPERIMENTAL SECTION

2.1. Experimental Setup. To prepare clear and bubble ice cubes, an experimental setup for icing is designed and constructed. As shown in Figure 1(a), the experimental setup consists of four systems, i.e., an icing system, a control system, a data acquisition system, and an auxiliary system. The icing system includes an icing chamber, a propeller, a heat exchanger, and a constant temperature bath. The icing chamber is a stainless steel shell that measures 16 cm in length, 16 cm in width, and 20 cm in height. To prevent heat loss during the icing process, insulating cotton is applied to the outside of the chamber. The propeller is submerged in the water to prevent trapped bubbles from forming in ice. The heat exchanger and the icing chamber are tightly connected and the joints are coated with thermally conductive silicone grease. The low-temperature glycol solvent in the thermostatic water bath removes heat from the icing chamber through the heat exchanger.

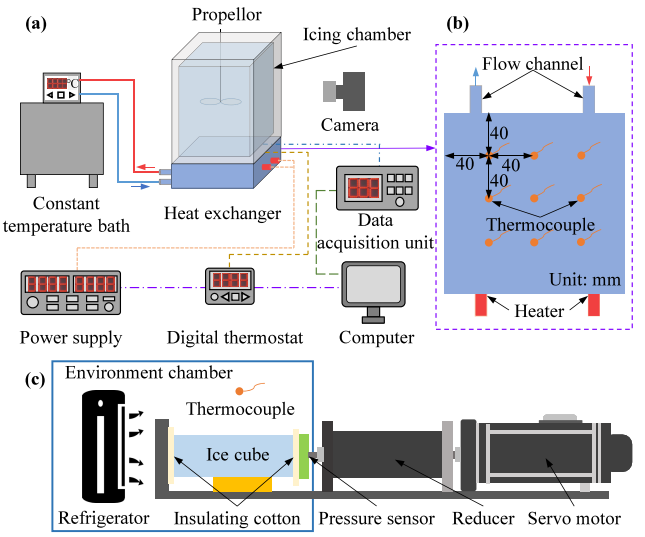

Figure 1. Schematic diagram of the experimental apparatus. (a) Schematic diagram of the experimental setup for ice-making. (b) Layout of thermocouples on the heat exchanger. (c) Schematic diagram of the experimental setup for ice mechanical strength measurement.

The control system consists of a digital thermostat, a power supply, and a heating rod. The digital thermostat indirectly controls the power of the heating rods by controlling the output power of the power supply to keep the icing temperature constant. The data acquisition system consists of an acquisition unit and thermocouples. The data acquisition unit is used to record the changes in values of the nine T-type thermocouples on the heat exchanger. The layout of the thermocouples is shown in Figure 1(b). Since the icing temperature affects the size and distribution characteristics of the bubbles in ice, the consistency of the icing temperature needs to be maintained during the preparation of ice samples. To monitor the surface temperature of the heat exchanger in real time, nine thermocouples are uniformly arranged.

The experiments on the mechanical properties of ice cubes are carried out using a homemade setup for measuring the mechanical properties of ice cubes, the schematic diagram of which is shown in Figure 1(c). The setup consists of three parts, i.e., a driving unit, a measuring unit, and a refrigeration unit. The driving unit consists of a servo motor and a reducer. The measuring unit consists mainly of a pressure sensor and a thermocouple. The refrigeration unit is a modified chiller. In addition, there is no standard for measuring the mechanical properties of ice, especially the size of the ice samples. Therefore, some scholars have studied the effect of the sample size on the mechanical strength of ice. This study mainly focuses on investigating the effect of trapped bubbles in ice cubes on different mechanical properties at different environmental temperatures. Therefore, it is sufficient to ensure that the dimensions of ice samples are the same under the same cases. To prevent the ice from melting during the measurement, the experiment needs to be performed in a low-temperature environment.[53,54] Both the control system and the data acquisition system are connected to a computer. Auxiliary systems include brackets and slide tables. The detailed parameters of these devices are listed in Table 1.[55]

2.2. Method and Materials. The specimens used in this study are prepared by the ice test device described in Section 2.1, where ice with different bubble volume contents can be prepared by controlling the rotational speed of the propeller.[55] The icing temperature is controlled more accurately due to the incorporation of an icing temperature control device in the icing apparatus of this experiment. The icing rates of clear and bubble ice tubes are shown in Figure 2. It can be seen that the time taken to prepare ice of the same height is 19,200 s and 22,200 s for clear and bubble ice cubes. During the first 4,000 s, stirring causes the water temperature to rise near the front

https://doi.org/10.1021/acsami.4c12227
ACS Appl. Mater. Interfaces 2024, 16, 63482−63494

Table 1. Details of the Main Device and Tools Used in This Study

No.	Equipment	Brand/Model	Parameter
1	Camera	Canon/EOS 90D	Resolution: 3840 pi × 2160 pi
2	Constant temperature bath	TENLIN/4006	Accuracy: ±0.2 °C
3	Data acquisition unit	Agilent/34972A	Frequency: ±2 Hz
4	Digital thermostat	Omron/E5CC	Accuracy: ±1 °C
5	Pressure sensor	HY/HYLF-010-2	Accuracy: ±1 N
6	Thermocouple	AiDIWEN/T	Accuracy: ±0.2 °C
7	Servo motor	SDCQ/23015	Accuracy: ±1 rpm

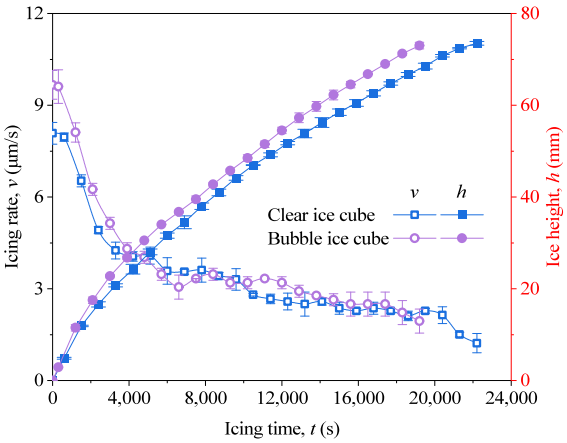

Figure 2. Variation of icing rate and height with time for clear and bubble ice cubes.

will prevent icing. After 4,000 s, the water temperature is lower, and thus the icing rate is almost equal to the icing rate for preparing a bubble ice cube. This is because the icing rate changes the size of the ice crystals, which affects the mechanical strength of the ice cube.[56] Therefore, to avoid the influence of ice crystal size on the strengths, the ice samples are all taken from the ice obtained by icing after 4,000 s.

To ensure the accuracy of the experimental results of the mechanical strength test of ice cubes, the homogeneity of all ice samples is to be ensured. The homogeneity of clear ice and bubble ice cubes is characterized using light transmittance and bubble volume content.[55] The detailed procedures and main device are described in Supporting Information Figures S1 and S2 and Table S1, and the results are shown in Figure 3. Results showed that the light

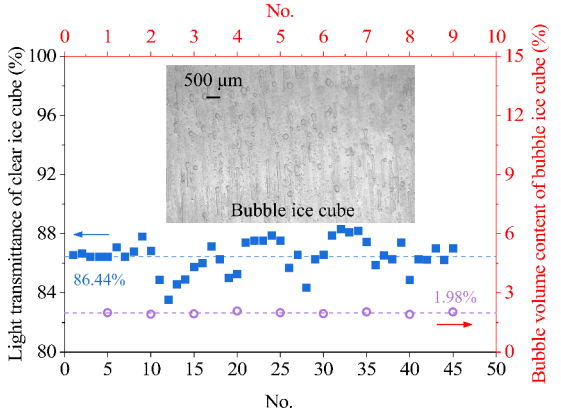

Figure 3. Characterization of the uniformity of clear and bubble ice cubes.

transmittance of each part of a piece of a clear ice cube with a length of 15 cm, a width of 15 cm, and a height of 7 cm is stable at about 86.44%, with a maximum error of less than 2%. The cause of less than 100% light transmittance in a clear ice cube may be the reflection of light on the grain boundary, resulting in a portion of the light changing its path. Ice is distributed with grains of different sizes and shapes, and grain boundaries exist between neighboring grains. When light passes through the grains, the grain boundaries reflect and refract part of the light.[57] The bubble volume content of each part of the same volume of the bubble ice cube is also around 1.98%, with a maximum error of less than 0.1%.

Four typical mechanical properties of ice cubes, i.e., tensile, compressive, bending, and shear strengths are measured at different environmental temperatures (T). Five temperatures are set which range from −20 to 0 °C at 5 °C intervals. To facilitate observation of the ice breakup process, the movement rate of the pressure sensor is set to 0.05 mm/s and thus a load (P) is exerted on the ice cube.[58,59] The principle of measurement for each mechanical strength is described in detail in previous literature.[60] The specific dimensions and expressions for calculating four typical mechanical properties of an ice cube are calculated as listed in Table 2.[55]

3. RESULTS

To investigate the effects of environmental temperature and trapped air bubbles on the mechanical properties of ice cubes, tensile, compressive, bending, and shear mechanical properties are chosen. The load−displacement curves of clear ice cubes at −10 °C are shown in Figure 4. Meanwhile, to further investigate the effects of environmental temperature and trapped air bubbles on them, the strength, stiffness, and modulus of ice cubes under different cases are analyzed. The strength reflects the maximum external stress that the ice can resist, and its value can be calculated from the maximum load (P_{max}). The slope of the load−displacement curve is defined as the stiffness (k) and characterizes the course of the ice cube under different operating conditions. The modulus reflects the degree of deformation of the ice cube under the loading force. The strength and modulus for different mechanical properties can be calculated using the equations listed in Table 2. In addition, the difference between the environmental temperature (T) and the freezing point (T_F) is defined as the relative environmental temperature, $T - T_F$.

3.1. Effect of Environmental Temperature and Trapped Bubbles on Strength. The strength best visualizes the extent to which bubbles affect the mechanical properties of an ice cube. The trend of tensile strength with relative environmental temperature for clear and bubble ice cubes is shown in Figure 5. The tensile strength of both types of ice increases with decreasing temperature. The tensile strength of bubble ice is significantly lower than that of clear ice cubes at the same temperature. For a clear ice cube, the tensile strength of clear ice at −20 °C is about 1.3 times that at 0 °C. For a bubble ice cube, the tensile strength at −20 °C is about 1.34 times that at 0 °C. It can be seen from Figure 5, that the effect of temperature on tensile strength is essentially linear. Based on this, the relationship between tensile strength and relative environmental temperature is fitted for both clear and bubble ice cubes. The slope of the fitted straight line reflects the sensitivity of the tensile strength of ice to the temperature. The slope of the fitted straight line for a clear ice cube is slightly larger than one of a bubble ice cube. This suggests that the tensile strength of a bubble ice cube is not as sensitive to changes in temperature as a clear ice cube is to changes in temperature. The slopes of the two straight lines differed by only 8.43%. This indicates that trapped bubbles weaken the

https://doi.org/10.1021/acsami.4c12227
ACS Appl. Mater. Interfaces 2024, 16, 63482−63494

Table 2. Ice Cube Dimensions and Expressions for Calculating Four Typical Mechanical Properties

No.	Item	Sketch	Ice cube size	Strength	Modulus
1	Tensile	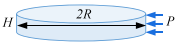	R = 50 mm, H = 30 mm	$\sigma_t = \frac{P_{max}}{\pi HR}$	$E_t = \frac{7P_{max}}{\pi H \Delta R}$
2	Compressive	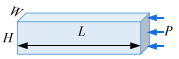	H = 30 mm, W = 30 mm, L = 65 mm	$\sigma_c = \frac{P_{max}}{HW}$	$E_c = \frac{\Delta \sigma_c}{\Delta H/H}$
3	Bending	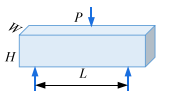	H = 30 mm, W = 30 mm, L = 150 mm	$\sigma_b = \frac{3LP_{max}}{2WH^2}$	$E_b = \frac{L^3 P_{max}}{4WH^3 \Delta H}$
4	Shear	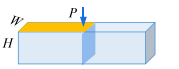	H = 30 mm, W = 30 mm,	$\sigma_s = \frac{P_{max}}{WH}$	$E_s = \frac{2\Delta \sigma_s}{\Delta H/H}$

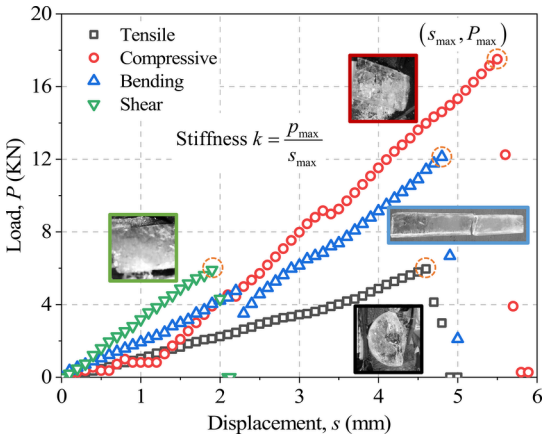

Figure 4. Load−displacement curves for ice cubes with different mechanical properties.

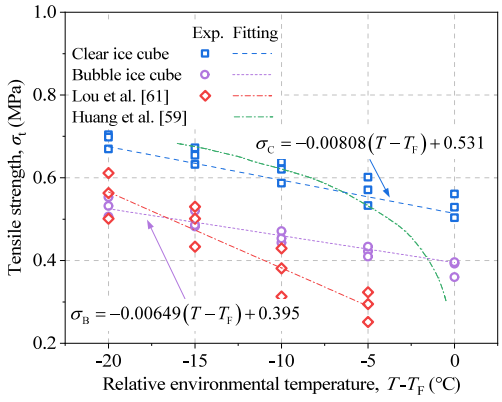

Figure 5. Tensile strengths of clear and bubble ice cubes at different environmental temperatures.

tensile strength of ice without affecting its deformation process. Furthermore, to verify the accuracy of this study, the experimental results are compared with those in the literature. Huang et al.[59] obtained the tensile strength of the ice to be somewhere in between that of the clear ice and the bubble ice cubes, while Lou et al.'s experimental results are slightly lower than the tensile strength of the bubble ice cubes.[61] The reason for this phenomenon is that the effect of trapped bubbles is neglected in their ice samples, resulting in a wide range of distribution of the obtained ice tensile strength.

The compressive strength of clear and bubble ice cubes at different relative environmental temperatures is shown in Figure 6. The compressive strengths of the two ice cubes increase gradually with the decreasing temperature. As the

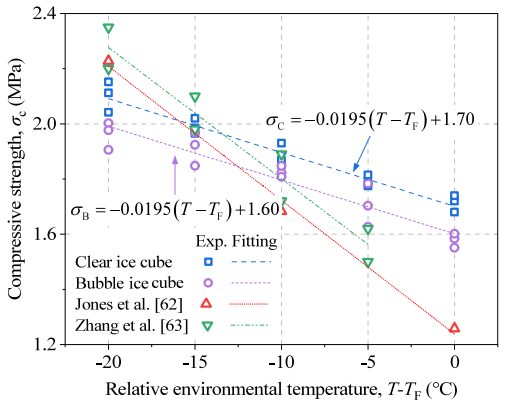

Figure 6. Compressive strengths of ice cubes at different environmental temperatures.

temperature decreases from 0 °C to −20 °C, the strength of the clear ice cube increases from 1.71 to 2.10 MPa, while one of the bubble ice cubes increases from 1.58 to 1.95 MPa. At 0 °C, the compressive strength of a clear ice cube is 1.08 times that of a bubble ice cube. At −20 °C, the compressive strength of a clear ice cube is 1.07 times that of a bubble ice cube. This indicates that the bubbles weaken the compressive strength of the ice cube but do not affect the deformation process. The difference in compressive strength between clear and bubble ice cubes shows a decreasing trend with increasing temperature. In addition, the experimental results of the present study are compared with those in the literature. The results of Jones and Zhang showed that the slope of the fitted straight line for the variation of ice compressive strength is greater than the slope of the fitted straight line obtained in this experiment.[62,63] The distribution of ice compressive strength at the same temperature has a wide range. The difference between the maximum and minimum values of ice compressive strength obtained by Zhang at −15 °C is 5.88%.

The bending strength of ice cubes at different relative environment temperatures is shown in Figure 7. It can be seen that the bending strength of both clear ice and bubble ice increases gradually with the decreasing temperature. When the temperature decreases from 0 °C to −20 °C, the strength of a clear ice cube increases from 2.06 to 2.42 MPa, while that of a bubble ice cube increases from 1.61 to 2.15 MPa. The bending strength of a clear ice cube is 1.28 times that of a bubble ice

https://doi.org/10.1021/acsami.4c12227
ACS Appl. Mater. Interfaces 2024, 16, 63482−63494

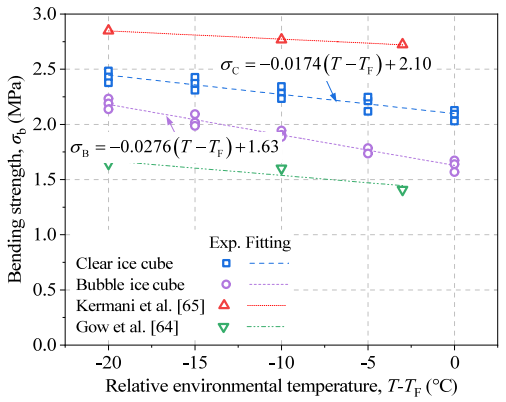

Figure 7. Bending strengths of clear and bubble ice cubes at different environmental temperatures.

cube at 0 °C, while the bending strength of a clear ice cube is 1.13 times that of a bubble ice cube at −20 °C. In addition, the slopes of the two lines differ by 53.34%. This indicates that the bubbles weaken the bending strength of the ice cube and also change the deformation process. As the temperature decreases. The difference in bending strength between clear and bubble ice cubes tends to diminish. The results obtained by different scholars for the bending strength of ice at different temperatures are also displayed in Figure 7.[64,65] It can be seen that the values of bending strength of bubble ice and clear ice cubes obtained in this experiment are within the range of the values obtained by other scholars. The reason for the wide range of distribution of the values of ice bending strength at the same condition in the literature may also be due to the different bubble contents of the ice samples used in experiments.

The shear strength of clear and bubble ice cubes at different relative environment temperatures is shown in Figure 8. The

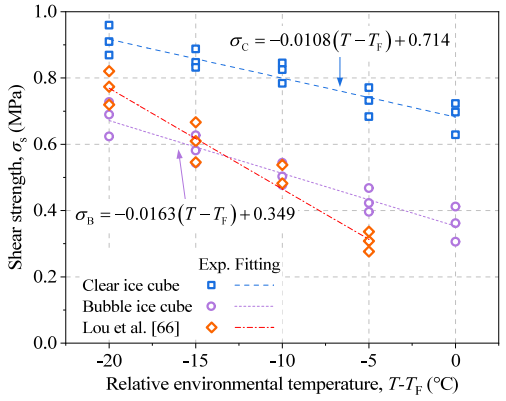

Figure 8. Shear strengths of clear and bubble ice cubes at different environmental temperatures.

shear strength of both clear and bubble ice cubes increases gradually with decreasing temperature. When the temperature decreases from 0 °C to −20 °C, the shear strength of a clear ice cube increases from 0.68 to 0.91 MPa, while the shear strength of bubble ice increases from 0.36 to 0.68 MPa. At 0 °C, the shear strength of the clear ice cube is 1.88 times that of the bubble ice cube. At −20 °C, the shear strength of the clear ice cube is 1.34 times that of the bubble ice cube. As the temperature decreases, the difference between them tends to decrease. In addition, the slopes of the two lines differ by 37.07%. This indicates that the bubbles weaken the shear strength of the ice cube and also change the deformation process. As the temperature decreases, the difference in shear strength between clear and bubble ice tends to decrease. This suggests that the effect of bubbles on the shear strength at low temperatures is less than the effect of the temperature. The range of ice shear strength at different temperatures obtained by Lou is large and all the values are smaller than the clear ice cube shear strength obtained in this experiment.[66] The range of variation is consistent with the range of variation in this study. This is because the ice used in their experiment is a bubble ice cube.

The influencing degree of trapped bubbles on the strengths is defined as $\varepsilon = (\sigma_B - \sigma_C)/\sigma_C$ where σ_B and σ_C are the strengths of the bubble and clear ice tubes. The influencing degrees of the tensile, compressive, bending, and shear strengths under different relative environmental temperatures are shown in Figure 9. Bubbles reduce the four mechanical

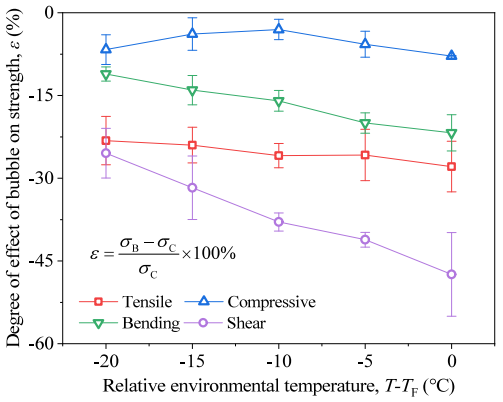

Figure 9. Effect of trapped bubbles on the stiffness at different environment temperatures.

properties, and the extent to which bubbles affect the four mechanical strengths decreases with decreasing temperature. Trapped bubbles have the greatest effect on shear strength and the least impact on tensile and compressive strengths. As the temperature decreases from 0 °C to −20 °C, the weakening of shear strength by bubbles decreases from 43.28% to 25.46%, while the weakening of tensile and compressive strength by bubbles changes from 27.89% to 23.18% and from 7.86% to 6.67%, respectively. Under compressive load, the bubble's spherical-shaped structure does a good job of spreading the force around the ice. Under shear loading, the bubble becomes the place where the stress is concentrated, causing the region to rupture first.

To better explain this phenomenon, the deformation of individual bubbles in a bubble ice cube at four different loads is obtained using numerical simulations and the results are presented in Figure 10. The detailed derivation process is shown in Supporting Information eqs S1−S3 and Tables S2 and S3. Ice is a brittle material whose compressive strength is greater than its tensile strength. Ice tends to undergo tensile damage when subjected to external forces.[67] Under tensile and compressive loads, the ice cube will fracture in the direction of the minor axis of the bubble. Under bending and shear loads, the ice cube will fracture in the direction of the major axis of the bubble. Due to the Gibbs−Thomson effect,[68,69] the freezing point of a substance decreases where the radius of curvature is large. Therefore, the freezing point of the ice cube on both sides of the major axis of the bubble will be lower than

https://doi.org/10.1021/acsami.4c12227
ACS Appl. Mater. Interfaces 2024, 16, 63482−63494

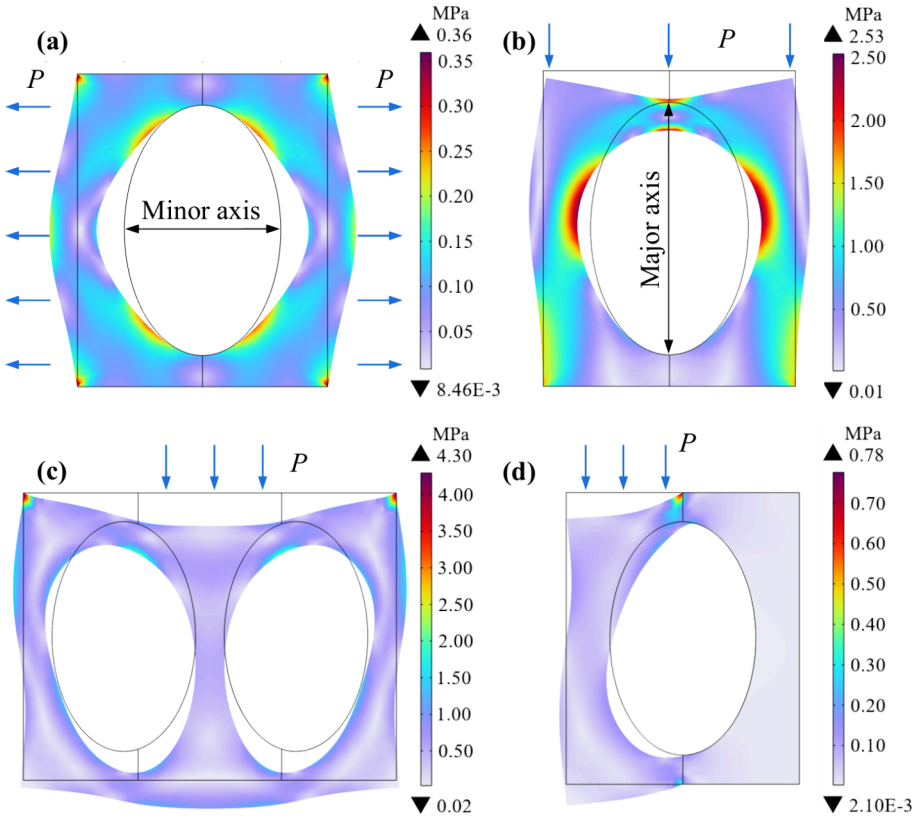

Figure 10. Deformation of a bubble ice cube under (a) tensile, (b) compressive, (c) bending, and (d) shear loads obtained from simulations.

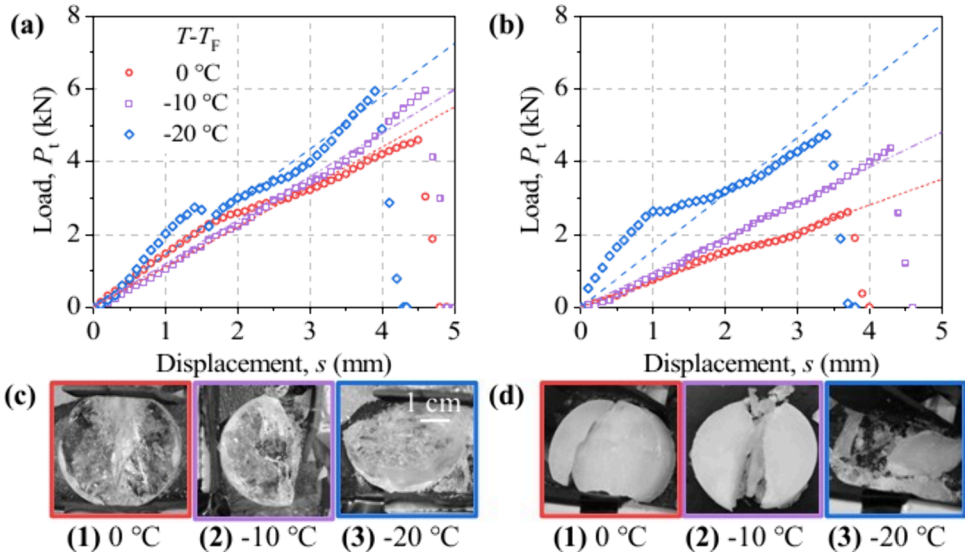

Figure 11. Results of clear and bubble ice cubes from tensile experimental load−displacement of (a) clear and (b) bubble ice cubes. Photos of (c) clear and (d) bubble ice cubes at different environmental temperatures.

the freezing point of the ice cube at other locations. The most destructive places of bubble ice under bending and shear loads are also located on both sides of the major axis of the bubble. Therefore, bending and shear strengths are more susceptible to temperatures.

3.2. Effect of Environmental Temperature and Trapped Bubbles on Stiffness. As shown in Figures 11(a) and 11(b), the maximum load of both types of ice cubes increases with the decreasing relative environmental temperature. The decrease in temperature increases the brittleness of the ice cube, thus increasing its resistance to stretching.[70] The load−displacement curves at −20 °C for both ice cubes are not a sloping straight line but have ripples in the middle part. The decrease in temperature increases the ice brittleness but also decreases the toughness of the ice cube. The internal rupture of the ice occurred under external forces, resulting in the ice no longer deforming elastically. The photos of ice after tensile damage are shown in Figures 11(c) and 11(d). The volume after ice cube destruction at −20 °C is less than that after ice destruction at 0 °C, especially bubble ice cube. This may be

https://doi.org/10.1021/acsami.4c12227
ACS Appl. Mater. Interfaces 2024, 16, 63482−63494

caused by bubbles increasing the brittleness of the ice cube. The slope of the load−displacement curve also increases with increasing relative environmental temperature. The stiffness of a clear ice cube is k_t = 1020.51 N/mm, 1301.11 N/mm, and 1519.74 N/mm at three temperatures, while the stiffness of a bubble ice cube is k_t = 701.11 N/mm, 1017.67 N/mm, and 1393.32 N/mm. Trapped air bubbles weaken the tensile stiffness of the ice, and the degree of weakening decreases with decreasing temperature.

To investigate the effect of trapped bubbles on the ice compressive process, the load−displacement curves of clear and bubble ice cubes at three different relative environmental temperatures are analyzed. As shown in Figures 12(a) and 12(b), the stiffness for both types of ice cubes increases with decreasing temperature. This may be because the increase in temperature improves the toughness of the ice cube. This can be verified by the fact that the lower the temperature the smaller the volume of the ice after it is destroyed as shown in Figures 12(c) and 12(d). The stiffness of k_c = 2548.09 N/mm, 3183.64 N/mm, and 3961.27 N/mm for clear ice cubes at the three temperatures are almost equal to that of k_c = 2301.09 N/mm, 3016.67 N/mm, and 3833.27 N/mm for bubble ice cubes under the same conditions. The difference in stiffness between the two types of ice at different temperatures is not more than 10%. Therefore, it can be assumed that temperature has no significant effect on the compressive stiffness of the ice cube.

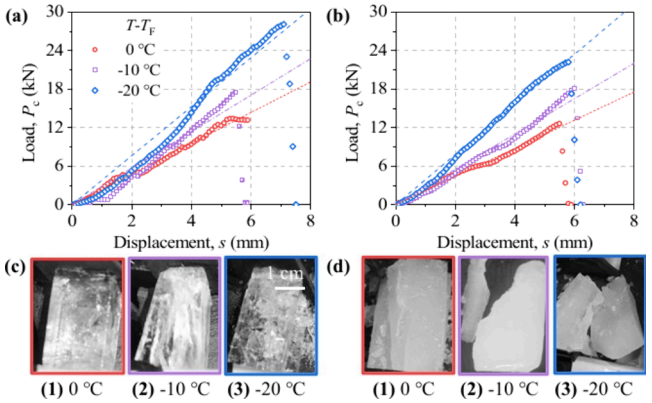

Figure 12. Results of clear and bubble ice cubes from compressive experimental load−displacement of (a) clear and (b) bubble ice cubes. Photos of (c) clear and (d) bubble ice cubes at different environmental temperatures.

To investigate the effect of trapped bubbles on the ice bending process, the load−displacement curves of clear and bubble ice cubes at three relative environmental temperatures are analyzed. As shown in Figures 13(a) and 13(b), the stiffness for both types of ice cubes increases with decreasing temperature. This may be because the increase in temperature increases the toughness of the ice cube. In addition, the stiffness of k_b = 166.766 N/mm, 251.64 N/mm, and 583.33 N/mm for clear ice cubes at the three temperatures is larger than that of k_b = 114.93 N/mm, 185.03 N/mm, and 279.06 N/mm for bubble ice cubes under the same conditions. The greater the stiffness, the stronger the ice cube's ability to resist load. The stiffness of a bubble ice cube under bending is less than that of a clear ice cube, which may be due to the many voids inside the bubble ice cube, which provide space for ice deformation. As seen from the photographs taken after the ice breakup in Figures 13(c) and 13(d), the bubbles have little effect on the breakup pattern.

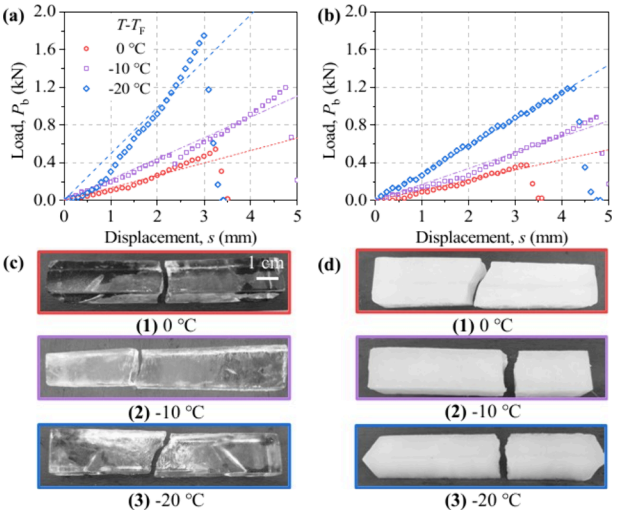

Figure 13. Results of clear and bubble ice cubes from bending experimental load−displacement of (a) clear and (b) bubble ice cubes. Photos of (c) clear and (d) bubble ice cubes at different environmental temperatures.

To investigate the effect of trapped bubbles on the ice shear process, the load−displacement curves of clear and bubble ice cubes at three relative environmental temperatures are analyzed. As shown in Figures 14(a) and 14(b), the stiffness for both types of ice cubes increases with decreasing temperature. The stiffness of k_s = 228.89 N/mm, 318.63 N/mm, and 547.58 N/mm for clear ice cubes at the three temperatures are greater than that of k_s = 80.4 N/mm, 135.71 N/mm, and 201.71 N/mm for bubble ice cubes under the same conditions. The stiffness of a clear ice cube under shear force is greater than that of the bubble ice cube, which may be because the bubbles inside the bubble ice cube become the place of stress concentration, rupture occurs at the bubbles under the stress and the cracks expand to other regions. This weakens the ability of the bubble ice cube to resist stress. As seen from the photographs taken after the ice breakup in Figures 14(c) and 14(d), the uneven section of the bubble ice cube also seems to indicate that the cracks have expanded in the ice resulting in less stiffness.

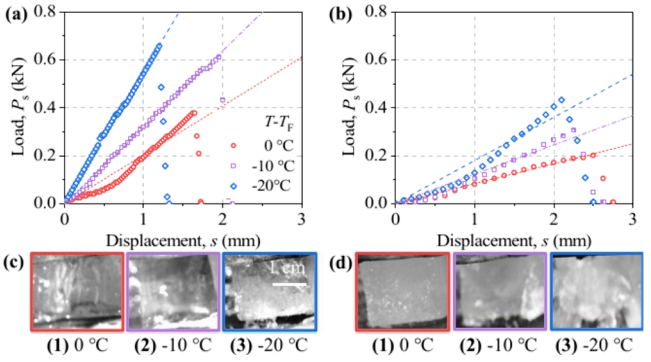

Figure 14. Results of clear and bubble ice cubes from shear experimental load−displacement of (a) clear and (b) bubble ice cubes. Photos of (c) clear and (d) bubble ice cubes at different environmental temperatures.

https://doi.org/10.1021/acsami.4c12227
ACS Appl. Mater. Interfaces 2024, 16, 63482−63494

To compare the influence of trapped bubbles on ice deformation under different environmental temperatures, the stiffnesses of ice cubes are also extracted from all the above load−displacement curves. The influencing degree of trapped bubbles on the stiffness is defined as $\eta = (k_B - k_C)/k_C$ where k_B and k_C are the stiffnesses of the bubble and clear ice tubes. The influencing degrees of the tensile, compressive, bending, and shear stiffnesses under different relative environmental temperatures are shown in Figure 15. Bubbles have the greatest

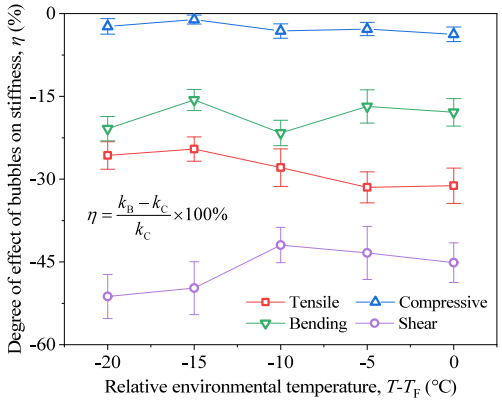

Figure 15. Effect of trapped bubbles on the stiffnesses at different environment temperatures.

impact on the shear, tensile, and bending stiffness, while they have the least impact on compressive stiffness. Compared to the clear ice cube, the shear, tensile, and bending stiffness of the bubble ice cube increases from 41.94% to 52.29%, 24.53% to 31.48%, and 16.82% to 21.63%, respectively, while the compressive stiffness increases slightly from 1.08% to 3.76%.

3.3. Effect of Environmental Temperature and Trapped Bubbles on Modulus. The tensile modulus of clear ice and bubble ice at different relative environmental temperatures is shown in Figure 16. As the temperature

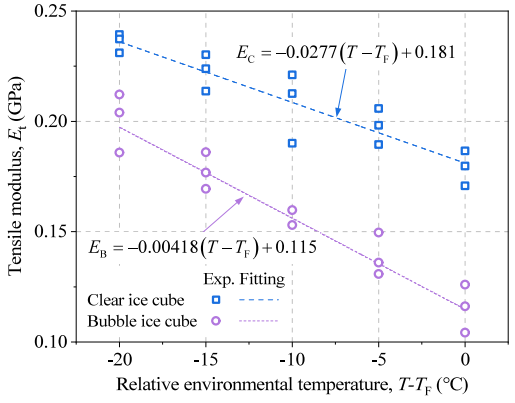

Figure 16. Tensile moduli of ice cubes at different environmental temperatures.

decreases, the tensile modulus of both types of ice increases linearly. The tensile modulus of a bubble ice cube is smaller than that of a clear ice cube at the same temperature. This is because trapped bubbles can disrupt the connections between ice crystals, leading to a decrease in the ice's ability to resist tensile deformation. The maximum tensile modulus of the clear ice cube is 0.236 GPa, while the maximum tensile modulus of the bubble ice cube is 0.177 GPa. The reason could be the different sizes and distribution of bubbles in the ice.

The compressive modulus of clear and bubble ice cubes at different relative environmental temperatures is shown in Figure 17. As the temperature decreases, the compressive

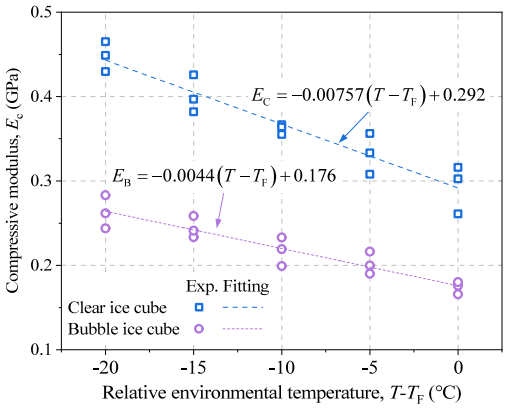

Figure 17. Compressive moduli of ice cubes at different environmental temperatures.

modulus of both types of ice cubes increases linearly. When the temperature decreases from 0 °C to −20 °C, the compressive modulus of a clear ice cube increases from 0.27 to 0.45 GPa, while the compressive modulus of a bubble ice cube increases from 0.17 to 0.26 GPa. This indicates that bubbles as defects in ice will reduce the ice's ability to resist compressive deformation. In addition, it also can be found that the influence of temperature changes on the compressive modulus of bubble ice cubes is smaller than that of the compressive modulus of clear ice cubes. This indicates that bubbles will limit the influence of temperature on the compressive modulus.

The bending modulus of clear and bubble ice cubes at different relative environmental temperatures is all shown in Figure 18. As the temperature decreases, the bending modulus of both types of ice cubes increases linearly. When the temperature decreases from 0 °C to −20 °C, the bending modulus of the clear ice cube increases from 0.89 to 1.19 GPa, while the compressive modulus of the bubble ice cube increases from 0.76 to 1.11 GPa. This indicates that bubbles as defects in ice will reduce the ice's ability to resist bending

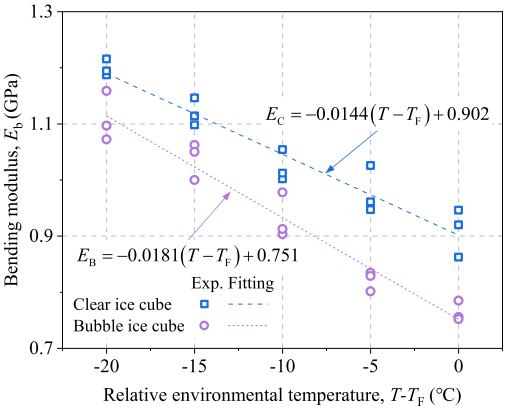

Figure 18. Bending moduli of ice cubes at different environmental temperatures.

https://doi.org/10.1021/acsami.4c12227
ACS Appl. Mater. Interfaces 2024, 16, 63482−63494

deformation. In addition, it can be found that the influence of temperature changes on the bending modulus of a bubble ice cube is smaller than that of the bending modulus of a clear ice cube. This indicates that bubbles will limit the influence of the temperature on the bending modulus of the ice cube.

The shear modulus of clear and bubble ice cubes at different relative environmental temperatures is all shown in Figure 19.

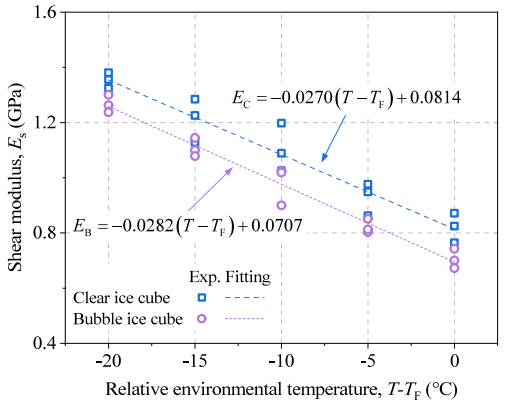

Figure 19. Shear moduli of ice cubes at different environmental temperatures.

As the temperature decreases, the shear modulus of both types of ice increases linearly. When the temperature decreases from 0 °C to −20 °C, the shear modulus of a clear ice cube increases from 0.76 to 1.41 GPa, while the compressive modulus of bubble ice increases from 0.67 to 1.26 GPa. This indicates that bubbles as defects in ice will reduce the ice cube's ability to resist shear deformation. In addition, it can be found that the influence of temperature changes on the shear modulus of a bubble ice cube is smaller than that of the shear modulus of a clear ice cube. This indicates that bubbles will limit the influence of the temperature on the shear modulus of an ice cube.

The influencing degree of trapped bubbles on the modulus is defined as $\zeta = (E_B - E_C)/E_C$ where E_B and E_C are the moduli of the bubble and clear ice tubes. The influencing degrees of the tensile, compressive, bending, and shear moduli under different relative environmental temperatures are shown in Figure 20. To explain the effect of temperatures on the different moduli, the stress distribution of bubbles under four

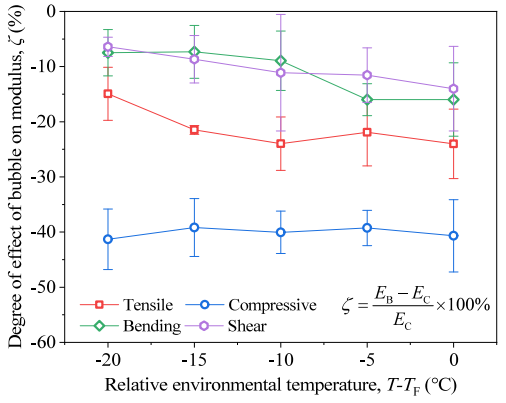

Figure 20. Effect of bubbles on the ice cube modulus at different relative environmental temperatures.

mechanics is simulated using numerical methods. As shown in Figure 10, the stresses on the bubbles in ice are mainly concentrated on the minor axis of the bubbles at the tension and compression process. This result is also consistent with the experimental observation of 45° shear damage in bubble ice cubes. In contrast, during bending and shearing, the stresses on the bubbles in ice are mainly concentrated on the major axis of the bubbles. This result is also consistent with the experimental observation that the bubble ice cube has a flat fracture surface. The Gibbs−Thomson effect suggests that where the radius of curvature is large, the freezing point of an object will be lower.[39,71] Thus, the freezing point at the ends of the major axis of a bubble is lower than the freezing point at the ends of the minor axis. The stresses are mainly concentrated on both sides of the minor axis at the tension and compression process. Therefore, the relative environmental temperature has little effect on the tension and compression process. The stress of the bubble is concentrated at the ends of the major axis of the bubble at the bending and shearing process, and the freezing point there is lower than that at other locations. Therefore, the relative environmental temperature affects their rupture process. As the temperature decreases, the positions on both sides of the major axis of the bubbles will be more prone to melting than other positions. This leads to a progressively more significant effect of bubbles on the mechanical properties of ice as the temperature decreases.

Both bubble ice and clear ice cube gradually increase their mechanical strength and modulus as the relative environmental temperature decreases. This is due to the low kinetic energy of atoms or molecules at low temperatures, which results in a relatively stable and highly ordered structure. This orderliness makes the internal structure of ice stronger, thus enhancing the strength of ice. In contrast, an increase in temperature leads to an increase in the relaxation and thermal movement of the ice crystal structure, which results in a weakening of the gravitational force between ice molecules and a disruption of the orderliness of the crystals. The high temperature also leads to an increase in the plasticity of ice, which is prone to plastic deformation. In addition, temperature also has a significant effect on the toughness of ice. At high temperatures, the plasticity of ice increases, and dislocation operation in the ice crystal structure is more likely to occur, thus increasing the toughness of ice. At low temperatures, dislocation movement in the ice crystal structure is difficult, and ice resistance to deformation increases, but ice fractures and breaks more quickly.

4. DISCUSSION

All four mechanical strengths of clear and bubble ice cubes are linearly related to the relative environmental temperature. To measure the weakening effect of trapped bubbles on the mechanical strength of an ice cube, the ratio of the strength of a bubble ice cube to that of a clear one under the same conditions is defined as C_T, which can be expressed as eq 1

$$C_T = \frac{\sigma_B}{\sigma_C} = f(T - T_F) = a_T(T - T_F) + b_T \quad (1)$$

where a_T and b_T are fitting coefficients and their values under different stress states from the experiments are listed in Table 3.

In addition, trapped bubbles also affect the mechanical strength of an ice cube. To measure the extent to which

https://doi.org/10.1021/acsami.4c12227
ACS Appl. Mater. Interfaces 2024, 16, 63482−63494

Table 3. Fitting Values of a_T and b_T under Different Stress States from Experiments

No.	Item	a_T	b_T
1	Tensile	0.0115	0.759
2	Compressive	0.00909	0.805
3	Bending	0.00758	0.901
4	Shear	0.0128	0.787

trapped bubbles affect the mechanical strength of an ice cube, a mathematical model relating the mechanical strength and the bubble volume content (φ) is developed. The detailed derivation process is shown in Supporting Information Figures S3−S8 and eqs S4−S25. At the same environmental temperature, the ratio of the strength of a bubble ice cube to that of a clear one is calculated by eq 2

$$C_B = g(\varphi) = a_B\varphi^{2/3} + b_B \tag{2}$$

where a_B is a fitting coefficient related to the shape and distribution of the bubble $b_B = 1$, and φ is the bubble volume content of the ice cube. Table 4 gives the concrete expressions

Table 4. Concrete Expressions of C_B from the Model and Fitting Value of a_B from Experiments

No.	Item	Expression of C_B	a_B
1	Tensile	$C_t = 1 - \frac{3^{2/3}\pi^{1/3}}{m_d^{1/3}(4\pi m_s)^{2/3}}\varphi^{2/3}$	3.5
2	Compressive	$C_c = 1 - \frac{3^{2/3}m_d^{2/3}\pi^{1/3}}{(4\pi m_s)^{2/3}}\varphi^{2/3}$	2.5
3	Bending	$C_c = 1 - \frac{3^{2/3}m_d^{2/3}(m_s\pi)^{1/3}}{4^{2/3}}\varphi^{2/3}$	2.2
4	Shear	$C_c = 1 - \frac{3^{2/3}m_d^{2/3}(m_s\pi)^{1/3}}{4^{2/3}}\varphi^{2/3}$	5.0

of C_B from the mathematical model and the fitting values of a_B from the experiments all under different stress states. Of note, m_s and m_d are the size and distribution coefficients of the trapped air bubbles in the ice cube, and their values are obtained from the fitting.

Both the relative environmental temperature and the bubble volume content affect the mechanical strength of the ice cube. Under their comprehensive influence, the ratio of the strength of a bubble ice cube to that of a clear one can be described as eq 3, which is obtained by combining eqs 1 and 2.

$$C = C_T C_B = f(T - T_F)g(\varphi) \tag{3}$$

Using the equation, Figure 21 presents the calculated and experimental ratios for the four mechanical strengths of ice cubes under various relative environmental temperatures and bubble content. The calculated and experimental values of the models for the effects of environmental temperature and trapped air bubbles on the mechanical strength of ice show a high degree of agreement, with the maximum deviation of the four models from the experimental values being less than 20%. The detailed comparative results are shown in the Supporting Information Figure S9.

5. CONCLUSIONS

To investigate the effects of environmental temperature and trapped air bubbles on the mechanical properties of ice cubes, a series of experimental cases are designed and carried out. A mathematical model that predicts the strength of an ice cube with an accuracy over 80% is developed and validated. The following conclusions are acquired:

(1) The relative environmental temperature decreases from 0 °C to −20 °C, the weakening of shear strength by bubbles decreases from 43.28% to 25.46%, while the weakening of tensile and compressive strength caused by

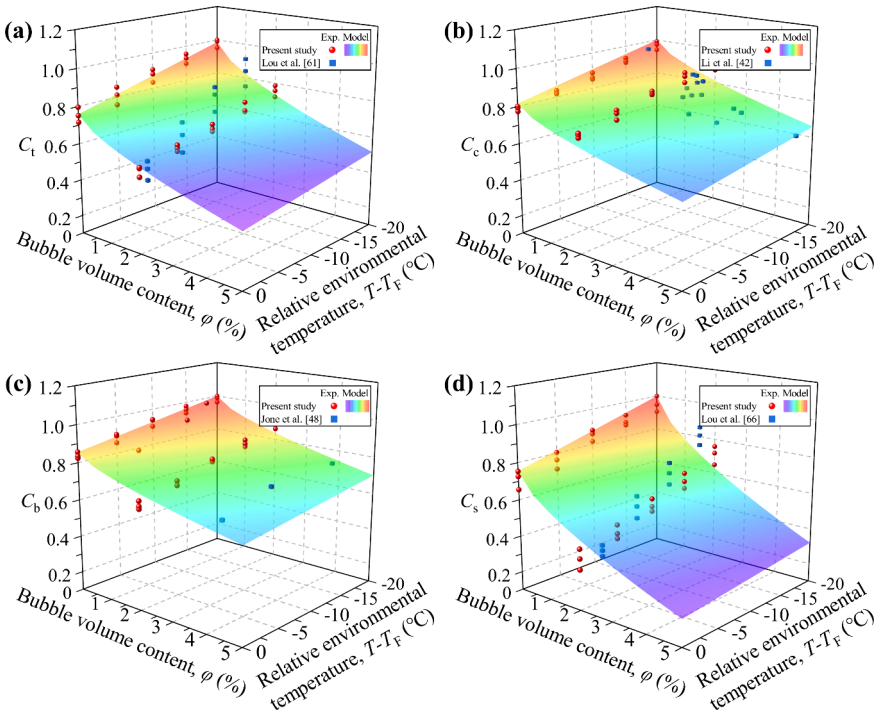

Figure 21. Calculated and experimental ratios of the bubble ice cube strength to the clear one for (a) tensile, (b) compressive, (c) bending, and (d) shear.

https://doi.org/10.1021/acsami.4c12227
ACS Appl. Mater. Interfaces 2024, 16, 63482−63494

bubbles changes from 27.89% to 23.18%, and from 7.86% to 6.67%, respectively.

(2) Compared to the shear, tensile, and bending stiffnesses of the clear ice cube, those of bubble ice cube increase from 41.94% to 52.29%, 24.53% to 31.48%, and 16.82% to 21.63%, respectively, while the compressive stiffness slightly increase from 1.08% to 3.76%.

(3) The effect of trapped air bubbles on the compressive modulus hardly varies with relative environmental temperature, while the tensile modulus is sensitive to relative environmental temperature. When the relative environmental temperature decreases from 0 °C to −20 °C, the effect of trapped air bubbles on the tensile modulus decreases from 24.01% to 19.17%.

(4) The deviation of the calculated and experimental values of the four mechanical strength prediction models is less than 20%. As the trapped air bubble volume content increases from 1% to 2%, the strength of the ice cube decreases by 7.24%, 15.02%, 13.87%, and 27.81% at 0 °C.

■ ASSOCIATED CONTENT

Data Availability Statement

Data will be made available on request.

Supporting Information

The Supporting Information is available free of charge at https://pubs.acs.org/doi/10.1021/acsami.4c12227.

Details of experiments for the measurement of light transmittance in clear ice cubes, details of experiments for the measurement of trapped air bubble volume content in bubble ice cubes, details of a numerical simulation method for the change in the shape of the bubbles under different stresses, and details of a model for the effect of environmental temperature and bubble volume content on the mechanical properties of ice cubes (PDF)

■ AUTHOR INFORMATION

Corresponding Authors

Mengjie Song − *Department of Energy and Power Engineering, School of Mechanical Engineering, Beijing Institute of Technology, Beijing 100081, China;* orcid.org/0009-0000-4234-626X; Email: mengjie.song@bit.edu.cn

Xuan Zhang − *Department of Energy and Power Engineering, School of Mechanical Engineering, Beijing Institute of Technology, Beijing 100081, China;* orcid.org/0000-0002-4999-7361; Email: xuan.zhang@bit.edu.cn

Authors

Keke Shao − *Department of Energy and Power Engineering, School of Mechanical Engineering, Beijing Institute of Technology, Beijing 100081, China*

Biaohua Cai − *Wuhan Second Ship Design and Research Institute, Wuhan 430205, China*

Long Zhang − *Department of Energy and Power Engineering, School of Mechanical Engineering, Beijing Institute of Technology, Beijing 100081, China*

Libor Pekař − *Faculty of Applied Informatics, Tomas Bata University in Zlín, 76005 Zlín, Czech Republic; Department of Technical Studies, College of Polytechnics Jihlava, 58601 Jihlava, Czech Republic*

Complete contact information is available at: https://pubs.acs.org/10.1021/acsami.4c12227

Notes

The authors declare no competing financial interest.

■ ACKNOWLEDGMENTS

This research is funded by the National Natural Science Foundation of China (Grant No. 52076013, No. 52406007, No. 52306003), the Beijing Municipal Science & Technology Commission (Grant No. 3212024, No. 324406, No. 3232032), the Key Laboratory of Icing and Anti/Deicing (No. IADL20230113 and No. IADL20220304), and the Young Elite Scientist Sponsorship Program by BAST (No. BYESS2023352).

■ REFERENCES

(1) Davis, A.; Yeong, Y. H.; Steele, A.; Bayer, I. S.; Loth, E. Superhydrophobic Nanocomposite Surface Topography and Ice Adhesion. *ACS Appl. Mater. Interfaces* **2014**, *6* (12), 9272−9279.

(2) Zhang, X.; Liu, X.; Wu, X. M.; Min, J. C. Impacting-Freezing Dynamics of a Supercooled Water Droplet on a Cold Surface: Rebound and Adhesion. *Int. J. Heat Mass Trans.* **2020**, *158*, 119997.

(3) Shi, H.; Yu, S. R.; Song, M. J.; Zhang, L.; Zhang, X. Experimental Study on the Technology Optimization of Clear Ice Thickness Detection on Horizontal Cold Plate Surface by Using Microwave Resonance. *Cold Reg. Sci. Technol.* **2024**, *228*, 104308.

(4) Yu, S. R.; Song, M. J.; Shen, J.; Sun, X. Q.; Wang, H. D.; Gao, R. M. Research Progress on Icing Characteristic Prediction Technologies for Low Temperature Stationary and Moving Surfaces. *Journal of Harbin Institute of Technology* **2024**, 1−19 (In Chinese).

(5) Shao, K. K.; Song, M. J.; Shen, J.; Zhang, X.; Pekař, L. Experimental Study on the Distribution and Growth Characteristics of Trapped Air Bubbles in Ice Slices at Different Freezing Temperatures. *Appl. Therm. Eng.* **2024**, *244*, 122600.

(6) Liu, Z. X.; Song, M. J.; Zhang, L.; Shao, K. K.; Zhen, Z. K.; Kim, D. R. Experimental Study on Heat Transfer Characteristics of Ice Melting Processes under Point-Source Bubble Flows. *Int. Commun. Heat Mass* **2024**, *159*, 108112.

(7) Rødland, E. S.; Okoffo, E. D.; Rauert, C.; Heier, L. S.; Lind, O. C.; Reid, M.; Thomas, K. V.; Meland, S. Road De-icing Salt: Assessment of a Potential New Source and Pathway of Microplastics Particles from Roads. *Sci. Total Environ.* **2020**, *738*, 139352.

(8) Machado, M.; Reilly, T.; Alvarado, V.; Ackerman, J.; Murohy, J.; Rice, W. Time-dependent Mechanical Response of Ice Adhesion on Aluminum Substrates. *ACS Appl. Mater. Interfaces* **2021**, *13* (12), 14662−14668.

(9) Yang, H. G.; Ma, C.; Li, K. Y.; Liu, K.; Loznik, M.; Teeuwen, R.; Hest, J. C. M.; Zhou, X.; Herrmann, A.; Wang, J. J. Tuning Ice Nucleation with Supercharged Polypeptides. *Adv. Mater.* **2016**, *28* (25), 5008−5012.

(10) Fu, D. Y.; Zheng, H. K.; Sheng, W.; Hao, X. R.; Zhang, X. M.; Chang, S. N.; Song, M. J. An Experimental Study on the Influence of Humidity on Ice Adhesion Strength on Superhydrophobic Surfaces with Microstructures. *Appl. Therm. Eng.* **2024**, *244*, 122732.

(11) Ahmadi, S. F.; Nath, S.; Iliff, G. J.; Srijanto, B. R.; Collier, C. P.; Yue, P. T.; Boreyko, J. B. Passive Antifrosting Surfaces Using Microscopic Ice Patterns. *ACS Appl. Mater. Interfaces* **2018**, *10* (38), 32874−32884.

(12) Sirui, Y.; Mengjie, S.; Runmiao, G.; Jiwoong, B.; Xuan, Z.; Shiqiang, Z. A review of icing prediction techniques for four typical surfaces in low-temperature natural environments. *Appl. Therm. Eng.* **2024**, *241*, 122418.

(13) Chu, F. Q.; Li, S. X.; Zhao, C. J.; Feng, Y. H.; Lin, Y. K.; Wu, X. M.; Yan, X.; Milijkovic, N. Interfacial Ice Spouting during Salty Water Droplet Freezing. *Nat. Commun.* **2024**, *15*, 2249.

(14) Meuler, A. J.; Smith, J. D.; Varanasi, K. K.; Mabry, J. M.; Mckinley, G. H.; Cohen, R. E. Relationships between Water

Wettability and Ice Adhesion. *ACS Appl. Mater. Interfaces* **2010**, *2* (11), 3100−3110.
(15) Gao, R. M.; Song, M. J.; Chao, C. Y. H.; Lin, S. L.; Zhang, L.; Zhang, X. Review on Condensation Frosting and Defrosting Experiments for Superhydrophobic Surfaces. *Appl. Therm. Eng.* **2024**, *236*, 121691.
(16) Rekuviene, R.; Saeidiharzand, S.; Mažeika, L.; Samaitis, V.; Jankauskas, A.; Sadaghiani, A. K.; Gharib, G.; Muganlı, Z.; Koşar, A. A Review on Passive and Active Anti-icing and De-icing Technologies. *Appl. Therm. Eng.* **2024**, *250*, 123474.
(17) Potter, R. S.; Cammack, J. M.; Braithwaite, C. H.; Church, P. D.; Walley, S. M. A Study of the Compressive Mechanical Properties of Defect-Free, Porous and Sintered Water-Ice at Low and High Strain Rates. *Icarus* **2020**, *351*, 113940.
(18) Matbou Riahi, M.; Marceau, D.; Laforte, C.; Perron, J. The Experimental/Numerical Study to Predict Mechanical Behaviour at the Ice/Aluminium Interface. *Cold. Reg. Sci. Technol.* **2011**, *65* (2), 191−202.
(19) Shao, K. K.; Song, M. J.; Zhang, X.; Kang, W. X.; Zhang, Y.; Zhang, L.; Liu, Y. X. A Review of Micro-scale Trapped Air Bubble Growth Distribution Characteristics and Thermal Mechanical Effects in Ice. *Journal of Harbin Institute of Technology* **2024**, *56* (6), 152 (In Chinese).
(20) Pandey, S.; Sharma, I.; Parameswaran, V. High Strain-Rate Behavior of Polycrystalline and Granular Ice: An Experimental and Numerical Study. *Cold. Reg. Sci. Technol.* **2024**, *227*, 104295.
(21) Sweidan, A. H.; Heider, Y.; Market, B. A Unified Water/Ice Kinematics Approach for Phase-Field Thermo-Hydro-Mechanical Modeling of Frost Action in Porous Media. *Comput. Method Appl. M.* **2020**, *372*, 113358.
(22) Kim, J. H.; Kim, Y.; Lu, W. J. Prediction of Ice Resistance for Ice-Going Ships in Level Ice Using Artificial Neural Network Technique. *Ocean Eng.* **2020**, *217*, 108031.
(23) Meng, D. D.; Chen, X. D.; Wei, Z. J.; Ji, S. Y. Prediction of Flexural and Uniaxial Compressive Strengths of Sea Ice with Optimized Recurrent Neural Network. *Ocean Eng.* **2023**, *288*, 115921.
(24) Petrovic, J. J. Review Mechanical Properties of Ice and Snow. *J. Mater. Sci.* **2003**, *38*, 1−6.
(25) Timco, G. W.; Weeks, W. F. A Review of the Engineering Properties of Sea Ice. *Cold Reg. Sci. Technol.* **2010**, *60* (2), 107−129.
(26) Rist, M. A.; Sammonds, P. R.; Murrell, S. A. F.; Meredith, P. G.; Oerter, H.; Doake, C. S. M. Experimental Fracture and Mechanical Properties of Antarctic Ice: Preliminary Results. *Ann. glacial.* **1996**, *23*, 284−292.
(27) Golding, N.; Schulson, E. M.; Renshaw, C. E. Shear Faulting and Localized Heating in Ice: The Influence of Confinement. *Acta Mater.* **2010**, *58* (15), 5043−5056.
(28) Schulson, E. M.; Gratz, E. T. The Brittle Compressive Failure of Orthotropic Ice under Triaxial Loading. *Acta Mater.* **1999**, *47* (3), 745−755.
(29) Schulson, E. M. The Brittle Failure of Ice under Compression. *J. Phys. Chem. B* **1997**, *101* (32), 6254−6258.
(30) Fallon, C.; Truyen, E.; Eakins, D.; Pervier, H.; Pervier, M. L. A.; Lopez, M. A. The Effect of Accretion Temperature on Microstructure and Bending Strength of Atmospheric Ice. *Mater. Today Commun.* **2023**, *37*, 107461.
(31) Arena, L.; Nasello, O. B.; Lebi, L. Effect of Bubbles on Grain Growth of Ice. *J. Phys. Chem. B* **1997**, *101*, 6109−6112.
(32) Azuma, N.; Miyakoshi, T.; Yokoyama, S.; Takata, M. Impeding Effect of Air Bubbles on Normal Grain Growth of Ice. *J. Struct. Geol.* **2012**, *42*, 184−193.
(33) Yoshimura, K.; Inada, T.; Koyama, S. Growth of Spherical and Cylindrical Oxygen Bubbles at an Ice-water Interface. *Cryst. Growth Des.* **2008**, *8* (7), 2108−2115.
(34) Dang, Q.; Song, M. J.; Zhang, X.; Zhang, L.; Shao, K. K.; Shen, J. Experimental Study about Solidification Process of Sessile Deformed Water Droplets on the Biaxial Inclined Cold Plate Surface under Natural Convection. *Appl. Therm. Eng.* **2024**, *236*, 121883.
(35) Carte, A. E. Air Bubbles in Ice. *Proc. Phys. Soc.* **1961**, *77*, 757−768.
(36) Xue, H.; Li, L. H.; Wang, Y. Q.; Lu, Y. H.; Cui, K.; He, Z. Y.; Bai, G. Y.; Liu, J.; Zhou, X.; Wang, J. J. Probing the Critical Nucleus Size in Tetrahydrofuran Clathrate Hydrate Formation Using Surface-anchored Nanoparticles. *Nat. Commun.* **2024**, *15*, 157.
(37) Dombrovsky, L. A.; Kokhanovsky, A. A. Solar Heating of Ice Sheets Containing Gas Bubbles. *J. Quant. Spectrosc. Ra.* **2020**, *250*, 106991.
(38) Wengrove, M. E.; Pettit, E. C.; Nash, J. D.; Jackson, R. H.; Skyllingstad, E. D. Melting of Glacier Ice Enhanced by Bursting Air Bubbles. *Nature* **2023**, *16*, 871−876.
(39) Shao, K. K.; Song, M. J.; Zhang, X.; Zhang, L. Growth and Distribution Characteristics of Trapped Air Bubbles in Ice Slices. *Phys. Fluids* **2023**, *35*, 113319.
(40) Bai, G. Y.; Gao, D.; Liu, Z.; Zhou, X.; Wang, J. J. Probing the Critical Nucleus Size for Ice Formation with Graphene Oxide Nanosheets. *Nature* **2019**, *576*, 437−441.
(41) Kovacs, A. Estimating the Full-Scale Flexural and Compressive Strength of First-year Sea Ice. *J. Geophys. Res.* **1997**, *102* (C4), 8681−8689.
(42) Li, Z. J.; Zhang, L. M.; Lu, P.; Leppäranta, M.; Li, G. W. Experimental Study on the Effect of Porosity on the Uniaxial Compressive Strength of Sea Ice in Bohai Sea. *Sci. China Technol. Sci.* **2011**, *54*, 2429−2436.
(43) Song, Z. H.; Hou, L.; Whisler, D.; Gao, G. F. Mesoscopic Numerical Investigation of Dynamic Mechanical Properties of Ice with Trapped Air Bubbles based on a Stochastic Sparse Distribution Mechanism. *Compos. Struct.* **2020**, *236*, 111834.
(44) Moslet, P. O. Field Testing of Uniaxial Compression Strength of Columnar Sea Ice. *Cold Reg. Sci. Technol.* **2007**, *48* (1), 1−14.
(45) Timco, G. W.; Frederking, R. Compressive Strength of Sea Ice Sheets. *Cold Reg. Sci. Technol.* **1990**, *17* (3), 227−240.
(46) Tang, E. L.; Liu, C.; Chang, M. Z.; Han, Y. F.; Chen, C. Influence of Freezing Temperature and Cotton Content of Ice on Dynamic Mechanical Properties and Energy Dissipation. *Eur. Phys. J. Plus* **2022**, *137*, 123.
(47) Zhang, X.; Li, K. L.; Liu, X.; Song, M. J.; Zhang, L.; Piskunov, M. Maximum Spreading of an Impact droplet on a Conical Tip. *Phys. Fluids* **2024**, *36*, No. 062110.
(48) Jones, S. J.; Chew, H. A. M. Effect of Sample and Grain Size on the Compressive Strength of Ice. *Ann. Glaciol.* **1983**, *4*, 129−132.
(49) Shazly, M.; Prakash, V.; Lerch, B. A. High Strain-rate Behavior of Ice under Uniaxial Compression. *Int. J. Solids Struct.* **2009**, *46* (6), 1499−1515.
(50) Douglass, R. G.; Palacios, J. L. Effects of Strain Rate Variation on the Shear Adhesion Strength of Impact Ice. *Cold Reg. Sci. Technol.* **2021**, *181*, 103168.
(51) Zhen, Z. K.; Song, M. J.; Shen, J.; Zhang, L.; Zhang, X. An Experimental Study on the Effect of CO_2 Laser Powers on Melting Characteristics of ice with Trapped Air Bubbles under Vertical Irradiation. *Appl. Therm. Eng.* **2024**, *236*, 121533.
(52) Maeno, N. Air Bubble Formation in Ice Crystals. *Phys. Snow Ice: proc.* **1967**, *1* (1), 207−218.
(53) Song, Z. H.; Chen, R.; Guo, D. L.; Yu, C. W. Experimental Investigation of Dynamic Shear Mechanical Properties and Failure Criterion of Ice at High Strain Rates. *Int. J. Impact Eng.* **2022**, *166*, 104254.
(54) Ma, D. Y.; Li, X.; Manes, A.; Li, Y. L. Numerical Modelling of Ice: Mechanical Behaviour of Ice under High Strain Rates. *Int. J. Impact Eng.* **2023**, *172*, 104375.
(55) Shao, K. K.; Zhen, Z. K.; Gao, R. M.; Song, M. J.; Zhang, L.; Zhang, X. Comparative Experimental Study of the Effect of Loading Rate on the Typical Mechanical Properties of Bubble and Clear Ice Cubes. *Exp. Therm. Fluid Sci.* **2024**, *159*, 111264.
(56) Masuda, H.; Ryuzaki, T.; Iyota, H. Role of Agitation in the Freezing Process of Liquid Foods Using Sucrose Aqueous Solution as a Model Liquid. *J. Food Eng.* **2022**, *330*, 111100.

(57) Di Prinzio, C. L.; Achával, P. I.; Aguirre Varela, G. G. Evolution of Crystalline Misorientations in Polycrystalline Samples of Pure Ice. *Chem. Phys.* **2024**, *582*, 112268.
(58) Deng, K.; Feng, X. W.; Tan, X. J.; Hu, Y. H. Experimental Research on Compressive Mechanical Properties of Ice under Low Strain Rates. *Mater. Today. Commun.* **2020**, *24*, 101029.
(59) Huang, S. B.; Liu, G.; Liu, F.; Xin, Z. K.; Cai, H. W. Experimental Investigation and Strength Model of Rough Ice-Filled Joints under Tensile and Shear Loading. *Eng. Geol.* **2023**, *325*, 107303.
(60) Meng, D. D.; Chen, X. D.; Wei, Z. J.; Ji, S. Y. Prediction of Flexural and Uniaxial Compressive Strengths of Sea Ice with Optimized Recurrent Neural Network. *Ocean Eng.* **2023**, *288*, 115921.
(61) Lou, X. N.; Wu, Y.; Huang, J. K.; Chen, Z. Q. The Tensile Mechanical Properties and Constitutive Model of Plain Ice and Fiber Reinforced Ice for Construction. *Constr. Build. Mater.* **2023**, *394*, 132050.
(62) Barrette, P. D.; Jordaan, I. J. Pressure-Temperature Effects on the Compressive Behaviour of Laboratory-Grown and Iceberg Ice. *Cold Reg. Sci. Technol.* **2003**, *36*, 25−36.
(63) Zhang, L. M.; Li, Z. J.; Jia, Q.; Huang, W. F. Experimental Study on Uniaxial Compressive Strength of Reservoir Ice. *Trans. Tianjin Univ.* **2012**, *18*, 112−116.
(64) Gow, J. A.; Ueda, T. H. Structure and Temperature Dependence of the Flexural Properties of Laboratory Freshwater Ice Sheets. *Cold Reg. Sci. Technol.* **1989**, *16*, 249−269.
(65) Kermani, M.; Farzaneh, M.; Gagnon, R. Bending Strength and Effective Modulus of Atmospheric Ice. *Cold Reg. Sci. Technol.* **2008**, *53* (2), 162−169.
(66) Lou, X. N.; Wu, Y. Influence of Temperature and Fiber Content on Direct Shear Properties of Plain Ice and Fiber-reinforced Ice. *Cold Reg. Sci. Technol.* **2022**, *194*, 103458.
(67) Snyder, S. A.; Schulson, E. M.; Renshaw, C. E. Effects of Prestrain on the Ductile-to-Brittle Transition of Ice. *Acta Mater.* **2016**, *108*, 110−127.
(68) Perez, M. Gibbs-Thomson Effects in Phase Transformations. *Scrpta Mater.* **2005**, *52* (8), 709−712.
(69) Makkonen, L. The Gibbs-Thomson Equation and the Solid-Liquid Interface. *Langmuir* **2002**, *18* (4), 1445−1448.
(70) Wei, P. C.; Zhuang, D. Y.; Zheng, Y. Y.; Zaoui, A.; Ma, W. Temperature and Pressure Effect on Tensile Behavior of Ice-Ih under Low Strain Rate: A Molecular Dynamics Study. *J. Mol. Liq.* **2022**, *355*, 118945.
(71) Jaafar, M. A.; Rousse, D. R.; Gibout, S.; Bédécarrats, J. A. A Review of Dendritic Growth during Solidification: Mathematical Modeling and Numerical Simulations. *Renewable Sustainable Energy Rev.* **2017**, *74*, 1064−1079.

https://doi.org/10.1021/acsami.4c12227
ACS Appl. Mater. Interfaces 2024, 16, 63482−63494